



ARCHIVES  
of  
FOUNDRY ENGINEERING

ISSN (2299-2944)  
Volume 18  
Issue 2/2018

163 – 168

DOI: 10.24425/122521

29/2



Published quarterly as the organ of the Foundry Commission of the Polish Academy of Sciences

# Dilatometric Research of High-quality Nodular Cast Iron

D. Medyński <sup>\*,a</sup>, A. Janus <sup>b</sup>

<sup>a</sup> Faculty of Technical and Economic Sciences, Witelon State University of Applied Science in Legnica, Sejmowa 5A, 59-220 Legnica, Poland

<sup>b</sup> Department of Foundry Engineering, Plastics and Automation, Wrocław University of Science and Technology, Smoluchowskiego 25, 50-372 Wrocław, Poland

\* Corresponding author. E-mail address: d.medyński.pwsz@interia.pl

Received 18.04.2018; accepted in revised form 08.06.2018

## Abstract

In the research, relationships between matrix structure and hardness of high-quality Ni-Mn-Cu cast iron containing nodular graphite and nickel equivalent value were determined. Nickel equivalent values were dependent on chemical composition and differences between them resulted mostly from nickel concentration in individual alloys. Chemical compositions of the alloys were selected to obtain, in raw condition, austenitic and austenitic-martensitic cast iron. Next, stability of matrix of raw castings was determined by dilatometric tests. The results made it possible to determine influence of nickel equivalent on martensite transformation start and finish temperatures.

**Key words:** Alloy cast iron, Austenitic cast iron, Dilatometry, Martensitic transformation, Nickel equivalent

## 1. Introduction

Higher and higher requirements imposed to cast iron castings more and more often induce designers to select high-quality cast iron with nodular graphite for machine parts. This results from the necessity to use the alloys characterised by higher strength combined with high abrasive-wear resistance and often also by increased corrosion resistance [1÷7].

According to the commonly dominating opinion, all structural components increasing hardness of cast iron at the same time increase its resistance to abrasive wear. From this viewpoint, chilled castings with martensitic matrix should show the highest resistance. However, in many cases, such a structure does not guarantee reaching the required minimum strength or also resistance to cracking. Much better results are obtained for non-chilled castings, containing in their structure, beside martensite, more plastic components. An example can be ausferritic structure of austempered ductile iron [1÷6].

In turn, high-alloy materials with one-phase matrix stabilised by elements having high electrochemical potential are characterised by increased corrosion resistance [7]. Among casting alloys, a typical representative of such materials is high-nickel cast iron Ni-Resist [8,9]. Austenitic matrix of this alloy guarantees high resistance to many corrosive environments, but does not assure suitably high resistance to abrasive wear.

An additional requirement that should be met by castings is their good machinability that is clearly worsened by hard acicular structures. For this reason, high hardness of cast iron should be reached during final heat treatment carried-out after machining of raw castings.

It seems that the above-mentioned requirements can be met by cast iron Ni-Mn-Cu containing nodular graphite, with properly chosen chemical composition. Selection of chemical composition is mostly based on nickel equivalent value  $E_{Ni}$  that considers influence of individual elements on stabilisation of austenite [7,10]:

$$\text{Equ}_{\text{Ni}} = 0.32 \cdot \text{C} + 0.13 \cdot \text{Si} + \text{Ni} + 2.48 \cdot \text{Mn} + 0.53 \cdot \text{Cu} \quad [\text{wt}\%], \quad (1)$$

where:

$\text{Equ}_{\text{Ni}}$  – nickel equivalent value [wt%],

C, Si, Ni, Mn, Cu – concentration of elements [wt%].

As was demonstrated by previous research works,  $\text{Equ}_{\text{Ni}}$  value is strictly related to structure and hardness of raw castings [7,10]. If the  $\text{Equ}_{\text{Ni}}$  value is higher than 16.0%, then structure of raw, non-chilled castings is composed of austenite only. As  $\text{Equ}_{\text{Ni}}$  is further increased over this value, thermodynamic stability of austenite increases. However, this restricts possibilities of such modification of raw casting matrix by heat treatment that it showed higher hardness and thus higher resistance to abrasive wear. In turn, when  $\text{Equ}_{\text{Ni}}$  is lower than 16.0%, partial transformation of austenite to martensite occurs during cooling-down in the mould. Percentage of martensite increases as the  $\text{Equ}_{\text{Ni}}$  value is decreased.

Higher percentage of martensite is accompanied by clearly higher hardness of castings. From the viewpoint of abrasive-wear resistance, this is a favourable phenomenon. However, at the same time it makes machining difficult or even impossible. Corrosion resistance of cast iron is also reduced, if lower  $\text{Equ}_{\text{Ni}}$  value results from lower concentration of nickel or copper.

So, it can be said that there exist such a chemical composition of nodular cast iron Ni-Mn-Cu, which, because of concentration of nickel and copper, ensures properly high corrosion resistance and hardness of raw castings that makes machining relatively easy. At the same time, structure of raw castings should be enough thermodynamically unstable that annealing of castings followed by relatively slow cooling would result in partial supersaturation of austenite to acicular ferrite strongly supersaturated with carbon.

However, degree of this transformation should be limited enough that sufficiently high tensile strength and impact strength of castings were maintained.

Table 1.

Chemical composition, nickel equivalent  $\text{Equ}_{\text{Ni}}$  and eutectic saturation ratio  $S_{\text{C}}$

Alloy No.	Chemical composition [wt%]								$\text{Equ}_{\text{Ni}}$ [wt%]	$S_{\text{C}}$ [ $\lambda$ ]
	C	Si	Ni	Mn	Cu	Mg	P	S		
<i>1</i>	3.1	2.3	<b>9.3</b>	2.4	2.4	0.12	0.16	0.04	<b>17.8</b>	1.08
<i>2</i>	3.3	2.3	<b>8.2</b>	2.3	2.5	0.09	0.16	0.04	<b>16.6</b>	1.13
<i>3</i>	3.4	2.3	<b>7.2</b>	2.5	2.4	0.11	0.15	0.03	<b>16.1</b>	1.13
<i>4</i>	3.4	2.2	<b>7.0</b>	2.4	2.5	0.13	0.16	0.04	<b>15.6</b>	1.13
<i>5</i>	3.3	2.3	<b>5.8</b>	2.4	2.4	0.10	0.15	0.03	<b>14.4</b>	1.08
<i>6</i>	3.3	2.2	<b>4.8</b>	2.3	2.4	0.12	0.15	0.03	<b>13.1</b>	1.05
<i>7</i>	3.3	2.1	<b>5.5</b>	<b>3.3</b>	2.3	0.10	0.15	0.03	<b>16.2</b>	1.04

Dilatometric examinations were carried-out on a vertical indirect dilatometer. Specimens were heated-up at 5°C/min till 800 °C. Next, at the same speed, the specimens were cooled-down to ambient temperature, then in vapours of liquid nitrogen to -150 °C and finally heated-up to ambient temperature. This way, the temperature loop of the measurement cycle was closed. For each

This means the necessity to determine the relationship between chemical composition ( $\text{Equ}_{\text{Ni}}$ ) and heat-treatment parameters of castings, and degree of austenite transformation. This paper is aimed at using dilatometric examinations to determine such a relationship.

## 2. Purpose, scope and methodology of the research

Examinations were carried-out on specimens coming from seven melts of cast iron, designated 1 to 7. The alloys 1 to 6 differed from each other mainly by nickel concentration. For comparative reasons, the additional alloy No. 7 was prepared, containing manganese as the main component stabilising austenite.

Cast iron for the examinations was smelted in a laboratory medium-frequency crucible furnace. For spheroidization, magnesium master alloy (CuMg17Ce1.1) and ferrosilicon (Si75T) were used. Test specimens were cut-out from Y-test ingots acc. to PN 76/H-83124, cast in bentonite moulding sand.

Chemical analysis was carried-out with use of a glow discharge analyser GDS 750 QDP and a scanning electron microscope Quanta FEI equipped with an EDX detector [3]. On these grounds, values of nickel equivalent  $\text{Equ}_{\text{Ni}}$  and eutectic saturation ratio  $S_{\text{C}}$  were calculated for each alloy. Results are given in Table 1.

Microscopic examinations were performed using a light microscope Eclipse MA200 and a scanning electron microscope TM 3000.

Brinell hardness of the castings was measured using a sintered carbide ball dia. 2.5 mm at 1838.75 N. Vickers microhardness of individual structural components was determined using a tester Nexus at 0.01N and 0.1N.

specimen, this cycle was repeated three times in order to determine repeatability of phase transformations occurring during subsequent heating and cooling of the examined specimens.

For each alloy, all tests were carried-out on at least three specimens.

### 3. Results and discussion

#### 3.1. Microscopic observations and hardness measurements

Microscopic observations performed on unetched polished sections showed correctly carried-out spheroidization process. In all alloys, precipitates of graphite with similar shape and arrangement (VI E acc. to EN-ISO 945-1:2009) were found. Content of graphite, determined as percentage on analysed surface of a polished section, was ca. 9% in all the alloys. However, for decreasing  $Equ_{Ni}$  values, slight decrease of graphite percentage was found, with concurrent increase of size of graphite particles – from No. 6 acc. to EN-ISO 945 for the alloy 1 to No. 5 for the alloy 6, see Fig. 1.

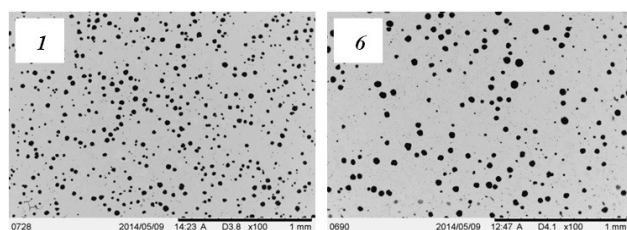


Fig. 1. Precipitates of graphite in the alloys No. 1 (VI E5) and No. 6 (VI E6). Unetched

Microscopic observations on etched polished sections showed strict connection of matrix structure and hardness of the castings with nickel equivalent value. Results of microscopic observations, hardness measurements and  $Equ_{Ni}$  values are given in Table 2.

In the alloys No. 1 to 3 and 7 ( $Equ_{Ni} > 16.0\%$ ), matrix structure was composed exclusively of austenite. Hardness of these alloys was similar, equal to  $168 \pm 200$  HBW. Small differences resulting from differences in microhardness of austenite ( $180 \pm 215$  HV0.01N) were related to differences in chemical composition.

In the alloys No. 4 to 6 ( $Equ_{Ni} < 16.0\%$ ), partial transformation of austenite was observed (Table 2 and Fig. 2). The created phase was strongly twinned, high-carbon ( $0.3 \pm 0.4\%C$ ) martensite with clearly visible habitus planes, see Fig. 3. Its microhardness was  $550 \pm 650$  HV0.1N.

Table 2.  
Nickel equivalent, composition of matrix and hardness of castings

Alloy No.	Composition of matrix	HBW	$Equ_{Ni}$ [wt%]
	$Fe_{\gamma} - Fe_m$ [% - %]		
1	100 – 0	186	17.8
2	100 – 0	174	16.6
3	100 – 0	168	16.1
4	94 – 6	231	15.6
5	79 – 21	296	14.4
6	64 – 36	373	13.1
7	100 – 0	200	16.2

$Fe_{\gamma}$  – austenite,  $Fe_m$  – martensite

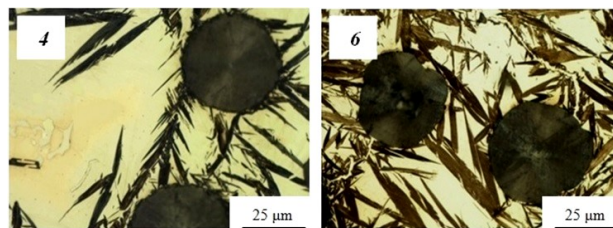


Fig. 2. Microstructure of Ni-Mn-Cu cast iron with nodular graphite: alloy No. 4 – low degree of austenite transformation to acicular phase and nodular graphite ( $Equ_{Ni} = 15.6\%$ ); alloy No. 6 – high degree of austenite transformation to acicular phase and nodular graphite ( $Equ_{Ni} = 13.1\%$ ). Etched with Mi1Fe

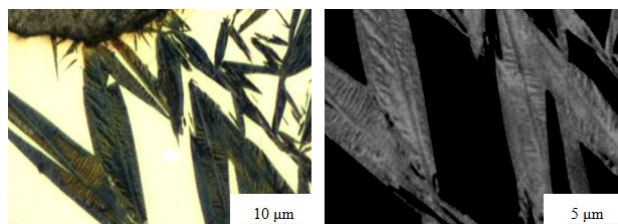


Fig. 3. Coarse needle-like martensite with visible habitus planes in the alloy No. 5 ( $Equ_{Ni} = 14.4\%$ ). Etched with Mi1Fe

Degree of austenite transformation in austenitic-martensitic cast iron increased with decreasing nickel equivalent value. Reduction of  $Equ_{Ni}$  value by 1% resulted in transformation degree higher in average by ca. 12%, see Fig. 4. At the same time, clearly higher hardness of castings was found, see Table 2. Relationship between  $Equ_{Ni}$  and hardness values of the examined castings is shown in Fig. 5. Therefore, additional melts were carried out, which were subjected to metallographic research. A obtained results were included in Fig. 5.

In the alloy with exclusively austenitic matrix ( $Equ_{Ni} > 16.0\%$ ), influence of nickel equivalent value on hardness of castings was small. Increasing  $Equ_{Ni}$  value by 1% resulted in increase of hardness by ca. 15 HBW only. As was stated before, that was caused by increased hardness of austenite.

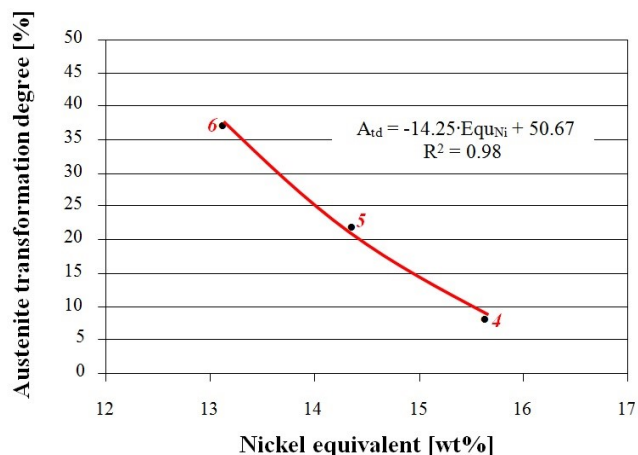


Fig. 4. Relationship between nickel equivalent value and austenite transformation degree (alloys 4 to 6)

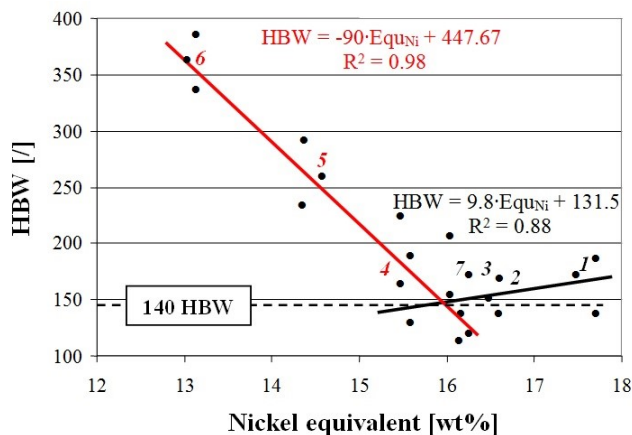


Fig. 5. Relationship between nickel equivalent value and hardness (alloys 1 to 7)

In turn, for austenitic-martensitic cast iron ( $Equ_{Ni} < 16\%$ ), increasing the  $Equ_{Ni}$  value by 1% resulted in reduction of hardness by ca. 80 HBW in average, reaching ca. 140 HBW at  $Equ_{Ni} \approx 16\%$ . The so distinct change of hardness resulted from strong relationship between  $Equ_{Ni}$  and degree of transformation of austenite to relatively hard martensite.

### 3.2. Dilatometric examinations

As previous examinations showed, annealing of austenitic cast iron ( $16.0\% < Equ_{Ni} < 18.0\%$ ) resulted in appearance of small amounts of martensite in the matrix [10]. Therefore, an attempt was made to determine stability of structures of raw castings by dilatometric measurements. The examinations were carried-out for cast iron with  $Equ_{Ni}$  ranging between 13.1% and 17.8%. Temperatures of start ( $M_s$ ) and finish ( $M_f$ ) of martensitic transformation were also determined.

Courses of dilatometric curves obtained in the first measuring cycle were significantly different from those obtained for the same specimens in the second and third cycles. Runs of the curves obtained in the second and third cycles were similar to each other. This regularity occurred irrespective of the  $Equ_{Ni}$  value, see Figs. 6 to 8.

Dilatometric curves obtained in the first cycle differed from each other. These differences were clearly related to structure of raw castings and thus to the  $Equ_{Ni}$  value.

In this paper, placed and exemplarily discussed are only the dilatograms for the alloys No. 1 (the highest  $Equ_{Ni}$  value), No. 4 ( $Equ_{Ni} \approx 16.0\%$ ) and No. 6 (the lowest  $Equ_{Ni}$  value), see Figs. 6 to 8.

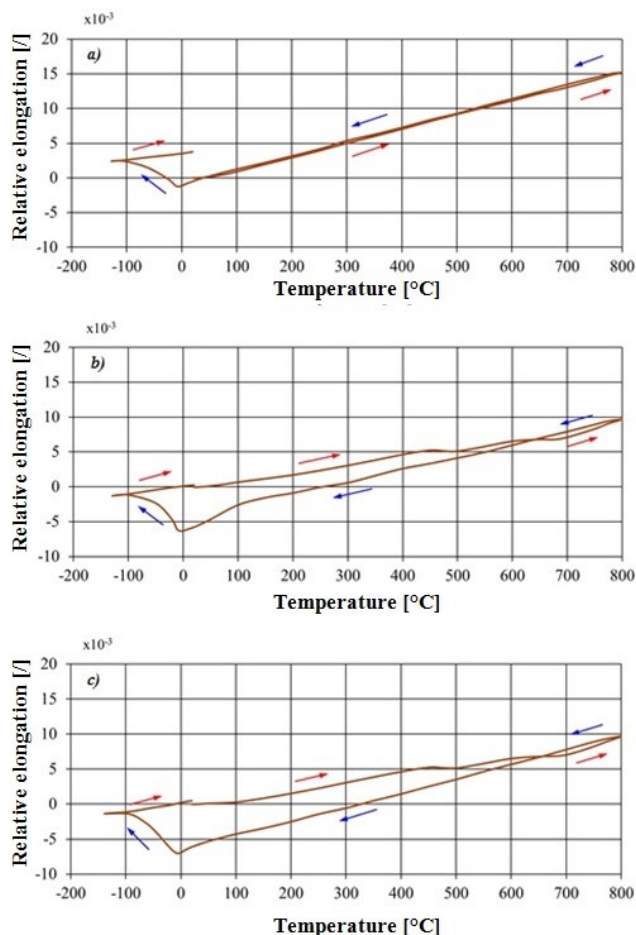


Fig. 6. Exemplary dilatograms for cast iron No. 1 ( $Equ_{Ni} = 17.8\%$ ) after: a) first; b) second and c) third measurement cycle

The dilatometric curve (1<sup>st</sup> cycle) obtained during heating-up cast iron No. 1 was rectilinear, see Fig. 6a. This evidences absence of structural changes. A similar run was obtained during cooling this specimen to ambient temperature. It is only freezing in vapours of liquid nitrogen (at  $-10\text{ }^\circ\text{C}$ ) that initiated martensitic transformation (demonstrated by increase of length with decreased temperature). Finish of the transformation (reduction of length with decreased temperature) occurred at  $-100\text{ }^\circ\text{C}$ . Examinations carried-out after heating to ambient temperature showed presence of martensite with hardness equal to  $460\text{--}500\text{ HV}0.1\text{N}$ .

During the second (Fig. 6b) and the third (Fig. 6c) heating cycle, martensite-austenite transformation began at ca.  $440\text{ }^\circ\text{C}$ .

Slow cooling did not cause austenite transformation till  $-5\text{ }^\circ\text{C}$ , at that martensitic transformation started. Its finish took place at  $95\text{ }^\circ\text{C}$ . After heating up to ambient temperature, austenitic transformation degree reached ca. 83%, see Fig. 9. At the same time, slight decrease of martensite hardness was found ( $450\text{--}470\text{ HV}0.1\text{N}$ ).

Shapes of the dilatograms obtained for the alloys No. 2, 3 and 7 were comparable. Values of  $M_s$  and  $M_f$  temperatures are given in Table 3.

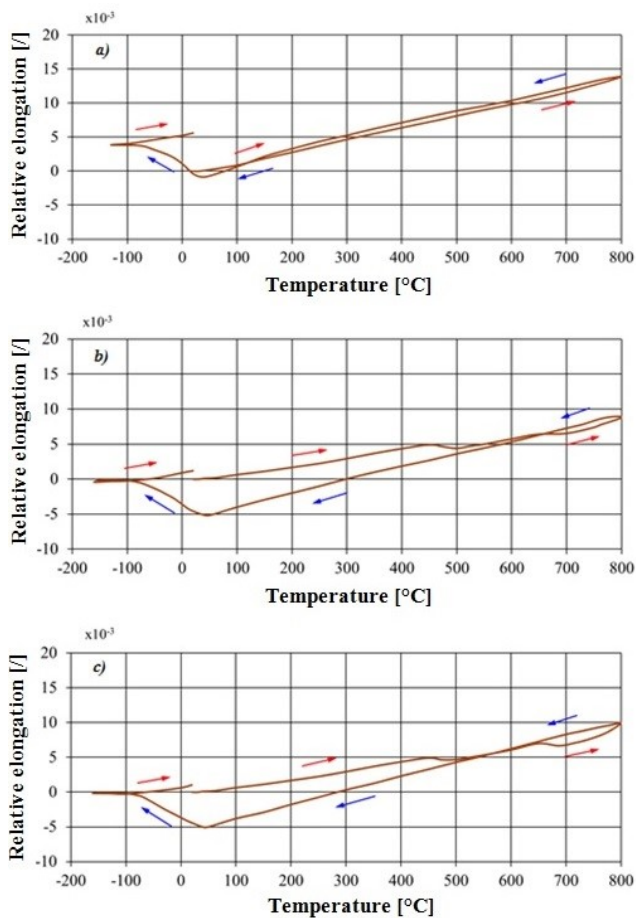


Fig. 7. Exemplary dilatograms for cast iron No. 4 ( $Equ_{Ni} = 15.6\%$ ) after: a) first; b) second and c) third measurement cycle

Even if a small amount of martensite was present in structure of the alloy No. 4 ( $Equ_{Ni} = 15.6\%$ ), its transformation during heating-up in the first measurement cycle did not cause any visible deviations from linear course of the dilatometric curve. Only after the amount of martensite increased as a result of heat treatment during the first measurement cycle, beginning of the transformation was clearly visible in subsequent heating cycles at 450 °C. Increased amount of martensite caused by the first measurement cycle is evidenced by sustained increase of length of the dilatometric specimen (Fig. 7) and the structure shown in Fig. 9. However, degree of austenite transformation was 95% and hardness of martensite ranged between 480 and 520 HV0.1N.

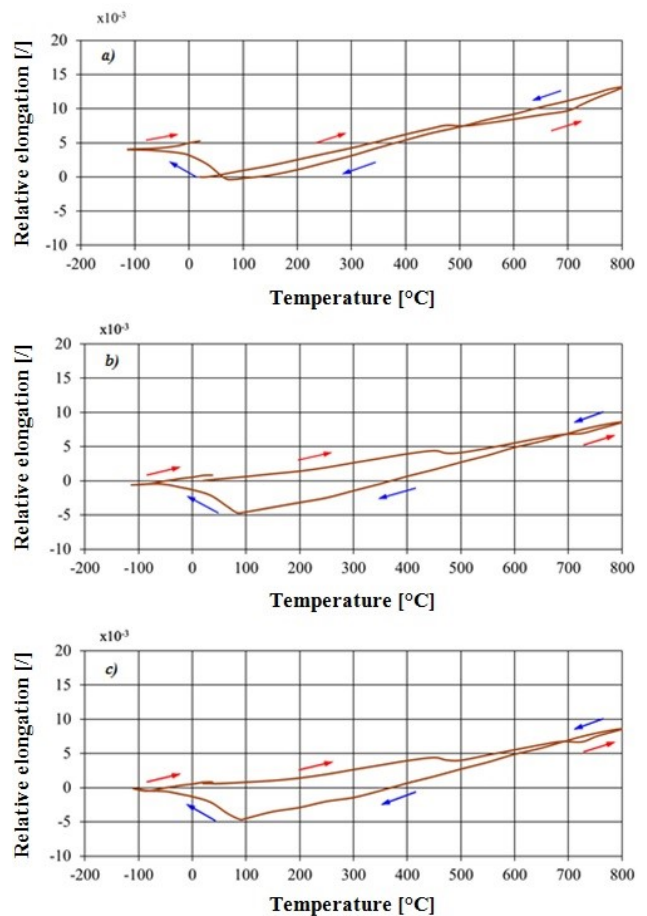


Fig. 8. Exemplary dilatograms for cast iron No. 6 ( $Equ_{Ni} = 13.1\%$ ) after: a) first; b) second and c) third measurement cycle

In the alloy No. 6 ( $Equ_{Ni}=13.1\%$ ), percentage of martensite in the structure was so big that a temperature stop is clearly visible on the heating curve of the first measurement cycle, indicating beginning of decomposition of martensite. Temperature range of this process is 480 to 700 °C (Fig. 8a).

During cooling, austenite was stable till 80 °C, after that martensitic transformation started. The transformation finished at -40 °C. Hardness of the created martensite was 600 to 640 HV0.1N.

In the subsequent measurement cycles, decomposition of martensite began at ca. 460 °C and lasted till ca. 700 °C, see Figs. 8b and 8c. During cooling, martensitic transformation started at 90 °C and finished at -55 °C.

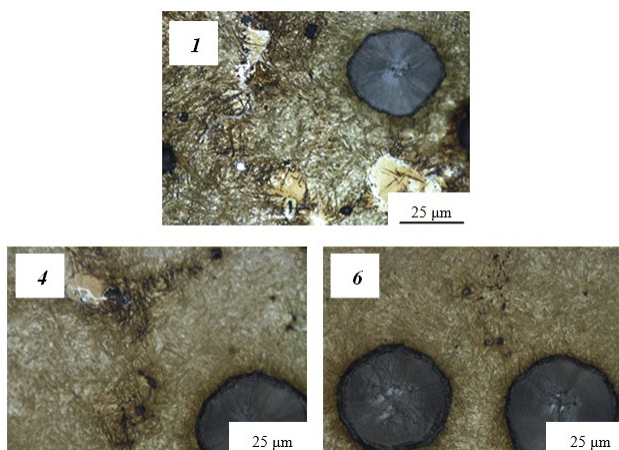


Fig. 9. Microstructure of the alloys No. 1, 4 and 6 after the third measurement cycle of dilatometric examinations. Etched with  $MiFe$

Reduction of the  $Equ_{Ni}$  value resulted in shifting the  $M_s$  and  $M_f$  temperatures towards higher values, see Table 3. Degree of these changes was larger for smaller values of the nickel equivalent. This was especially noticeable for the cast iron with  $Equ_{Ni} < 16.0\%$ .

Moreover, between the first and the next measurement cycles, a small shift of the  $M_s$  and  $M_f$  temperatures towards lower values was found for the same specimens.

Table 3.

Nickel equivalent  $Equ_{Ni}$ , temperatures of start  $M_s$  and finish  $M_f$  of martensitic transformation

$Equ_{Ni}$ [wt%]	Temperature [°C]					
	$M_s$			$M_f$		
	1st cycle	2nd cycle	3rd cycle	1st cycle	2nd cycle	3rd cycle
17.8	-10	-5	-6	-100	-95	-96
16.6	10	20	19	-90	-88	-88
16.2	20	29	30	-87	-82	-82
16.1	25	30	30	-85	-82	-81
15.6	30	36	35	-80	-80	-80
14.4	44	50	50	-70	-60	-61
13.1	80	90	89	-40	-55	-56

## 4. Summary and conclusions

The performed dilatometric examinations showed occurrence of a strict relationship between value of nickel equivalent and structure of a raw casting and thermodynamic stability of its structure. The examinations confirmed also that structures and properties of castings can be significantly changed by heat treatment (bringing to martensitic transformation). This heat treatment is represented by the first measurement cycle. However, it should be stressed here that, with the assumed range of  $Equ_{Ni}$

values (13.1–17.8%) and the assumed course of dilatometric measurements, bringing martensitic transformation to its end required cooling-down the specimens to a temperature much lower than 0 °C.

The examinations showed that reduction of the  $Equ_{Ni}$  value resulted in increasing both  $M_s$  and  $M_f$  temperatures. For this reason, temperature  $M_s$  was lower than 0 °C for the alloy No. 1 only.

If the first measurement cycle treated as heat treatment of raw castings brought to a change of the castings structure (evidenced by durable increase of length of dilatometric specimens), repeating the measurement did not result in significant structural changes. Dilatometric curves of the second and the third measurement cycles, obtained for individual alloys, basically did not differ between each other. This can indicate that the structures observed after heat treatment reached high thermodynamic stability. This also means that, when working at changing temperatures, castings made of such cast iron should not change their structure and properties.

## 5. References

- [1] Chang, C.H. & Shih, T.S. (1994). Study on isothermal transformation of austempered ductile iron. *AFS Transactions*. 94 (102), 357-385.
- [2] Zammit, A., Abela, S., Wagner, L., Mhaede, M. & Grech, M. (2013). Tribological behaviour of shot peened Cu-Ni austempered ductile iron. *Wear*. 302, 829-836.
- [3] Zhang, J., Zhang, N., Zhang, M., Liantao, L. & Zeng, D. (2014). Microstructure and mechanical properties of austempered ductile iron with different strength grades. *Materials Letters*. 119, 47-50.
- [4] Fatahalla, N. & Hussein, O. (2015). Microstructure, mechanical properties, toughness, wear characteristics and fracture phenomena of austenitized and austempered low-alloyed ductile iron. *Open Access Library Journal*. 2, 1-16.
- [5] Junjun, C. & Liqing, C. (2017). Microstructure and abrasive wear resistance of an alloyed ductile iron subjected to deep cryogenic and austempering treatments. *Journal of Materials Science & Technology*. 33, 1549-1554.
- [6] Sellamuthu, P., Harris Samuel, D.G., Dinakaran, D., Premkumar, V.P., Li, Z. & Seetharaman, S. (2018). Influence of austempering temperature on microstructure, mechanical and wear properties and energy consumption. *Metals*. 8(1), 53.
- [7] Medyński, D. & Janus, A. (2016). Effect of austenite transformation on abrasive wear and corrosion resistance of spheroidal Ni-Mn-Cu cast iron. *Archives of Foundry Engineering*. 16(3), 63-66.
- [8] Nickel Mond Company. *Ni-Resist Austenitic Cast Iron. Properties and Applications* (1962). London
- [9] Podrzucki, C. (1991). *Cast iron. Structure, properties and application*. T 1/2. Kraków: Ed. by ZG STOP. (in Polish).
- [10] Medyński, D., Janus, A. & Chęcmanowski, J. (2017). Effect of annealing on nature of corrosion damages of medium-nickel austenitic cast iron. *Archives of Foundry Engineering*. 17(3), 85-90.